MORPHOLOGICAL, THERMAL AND ELECTRICAL STUDIES ON CHITOSAN HEAVY METAL COMPLEXES

M. H. M. HUSAIN[1*], M. F. EL-HADY[2], W. M. SAYED[1], AND H. H. H. HEFNI[1]

1- Polymer lab, Petrochemicals Department, Egyptian Petroleum Research Institute (EPRI).

2- Chemistry Department, Faculty of Science, Al-Azhar University, Cairo-Egypt.

* mhmh43@hotmail.com

Abstract

The chitosan was prepared and mixed with some metal salts ($FeCl_3$, $Co(CH_3COO)_2$ and $NiCl_2$) with different concentrations to form chitosan-metal complexes. The characterizations of these complexes were carried out by FTIR and their morphological studies were carried out by scanning electron microscope (SEM) and wide angle X-ray diffraction apparatus. The thermo gravimetric analysis (TGA) and differential scanning calorimetric (DSC) also were carried out. The metal ions which strongly complexed to the amino groups of chitosan like Fe^{++} showed a smooth surface product, amorphous phase and thermally more stable than other complexes. The chitosan-metal complexes have a higher electrical conductivity than chitosan compounds at room temperature.

Keywords: chitosan, electrical conductivity, metal complex, morphology.

Introduction

Chitosan is a polymer of β-l,4-1inked 2-amino-2-deoxy- D-glucopyranose. It has been used extensively for various industrial and medical applications. It can be either derived by deacetylation of chitin or obtained from the cell walls of living organisms such as *Phycomyces blakesleeanus*. The contamination of water by heavy metal ions is a serious environmental problem, mainly due to the discarding of industrial wastes [1,2]. Heavy metals are highly toxic even when present in low concentrations and can accumulate in living organisms, causing several disorders and diseases [3-5]. Metals can be distinguished from other toxic pollutants, since they undergo chemical transformations, non-biodegradable, and have great environmental, economic, and public health impacts [6, 7]. One of the known properties of chitosan is its ability to complex strongly with heavy metal ions, especially with Fe^{2+}, Co^{2+}. Several applications of the product were proposed especially in water purification for the removal of toxic metals by complexation.

Experimental

Preparation of chitosan

The Shrimp shells were deproteinized with 3.5% (w/w) NaOH solution for 2 hr at 65ºC, and demineralized with 1N HCl for 1 day at ambient temperature and

subsequently decolorized with acetone for 2 hr at 50ºC and dried for 2 hr at ambient temperature.

The removal of acetyl groups from the prepared chitin was achieved by mixing with NaOH (50%) with stirring for 2 hr at 115ºC in a solid to solvent ratio of 1:10 (w/v). The resulting chitosan was washed till neutrality in running tap water, rinsed with distilled water, filtered, and then dried at 60ºC for 24 hr.

Preparation of chitosan–metal ($NiCl_2$, $FeCl_3$, $Co(CH_3COO)_2$) complexes.

5gm chitosan was dissolved in an aqueous solution of 10% V/V HCl by vigorous stirring to obtain 5% solution. Filtered through polyester cloth to remove residues of insoluble particles, the desired amount of metal ions (1/1, 1/2 and 1/3 mol metal ions/mol amino group of chitosan) were dissolved in 60 ml of 0.1 M HCl and added to chitosan solution. After agitation for 2hr at 60ºC the resulting homogeneous solution of the chitosan metal complex was added dropwise to a 0.5 M solution of NaOH. The resulting particles were filtered, washed several times with distilled water until pH 7, and dried in air for 48 h. the color of Ch-Ni is green, Ch-Fe is red and the Ch-Co is brown.

Characterization of chitosan and chitosan–metal ($NiCl_2$, $FeCl_3$, $Co(CH_3COO)_2$) complexes.

The elemental analysis of chitosan and their derivatives were carried out using CHNS/O analyzer (Perkin-Elmer, USA).

FT-IR spectra were recorded in the wave number range of 400 to 4200 Cm^{-1} with a resolution of 100 cm^{-1}.

The XRD analysis was carried out in an X-ray diffractometer (D/Max2500VB2+/Pc, Rigaku Company, Tokyo, Japan) with a Cu detector using 1.54 Aº wavelength of the X-Ray.

The thermo gravimetric analysis (TGA) and differential scanning calorimetric (DSC) measurements were carried out using a Netzsch DSC 204 (Germany). Polymer samples were heated under nitrogen atmosphere from 0°C to 700°C at a constant rate of 5 K/min.

The DC conductivity was measured with Keithly instrument high resistance model (6524 product information, March 2007), the samples were prepared in

pellets with 1cm diameter to obtain polymer powders by micrometer (Model 293-766; Mitutoyo, Tokyo, Japan).

The pellet was placed between the sample holder made from copper metal and the data were recorded at 295°K.

The morphology was determined using a scanning electron microscopy (SEM, TOPCON ABT150S, Japan). All samples coated with gold prior to analysis by SEM.

Results and Discussion

Preparation of chitosan metal ion complexes [8]

The reactions of chitosan with different ratios of metal ions were done at 60°C, with stirring for 2 hr. The chitosan metal complexes were produced in various forms according to metal ratios. Figs.1-3 show chitosan-metal complexes in molar ratio 1:1 Ch-M(1), 1:0.5 Ch-M(2), and 1:0.25 Ch-M(3) mole amino group of chitosan: mole metal ions.

Fig. 1 Reaction of chitosan and metal ions in a ratio 1:1of Ch-M(1)

Fig. 2 Reaction of chitosan and metal ions in a ratio 1:0.5 of Ch-M(2)

Fig. 3 Reaction of chitosan and metals ions a ratio 1:0.3 of Ch-M(3)where M is Fe^{3+}, Ni^{+2}, Co^{2+} and n is 2 or 3

The infrared spectra (FTIR)

Fig.4 shows the FTIR spectra of the prepared chitosan and chitosan-metal complexes, a strong and broad band at 3425 cm^{-1} is attributed to OH asymmetrical stretching vibration and NH_2 stretching vibrations; the $–CH_2$ bending at 1420 cm^{-1} and the absorption band at 1072 cm^{-1} is C-O-C stretching vibration in glucosidic linkage [9].

While the IR spectra of Ch-Fe complex showed; 3430 cm^{-1}-OH,-NH_2; 2922cm^{-1} and 2854 cm^{-1} -C-H stretching; 1634 cm^{-1} -C=O, amide; 1601cm^{-1} (-N-H amide); 1424cm^{-1} (-CH_2-N) coupled with 1379 cm^{-1} (-N-H); 1157cm^{-1} (skeleton: C-O and –C-O-C) ; 894 cm^{-1} C-O-C bridge as well as glucosidic linkage; 567 cm^{-1} (Fe-N-); 433 cm^{-1} (Fe-O-).

The IR spectra of Ch-Co complex; 3433cm^{-1}(-OH,-NH); 2921cm^{-1} and 2855 cm^{-1} (-C-H); 1626 cm^{-1} (-C=O, amide I); 1459cm^{-1} (-CH_2-N-) coupled with 1381 cm^{-1} (-N-H); 1113cm^{-1} (skeleton: C-O and –C-O-C);856 cm^{-1} C-O-C bridge as well as glucosidic linkage;556 cm^{-1} (Co-N-) ;451 cm^{-1}(Co-O-)[10].

The IR spectra of Ch-Ni complex; 3431 cm^{-1}(-OH,-NH_2); 2924cm^{-1} and 2859 cm^{-1} -C-H stretching; 1635 cm^{-1} -C=O, amide; 1462 cm^{-1} (-CH_2-N-) coupled with 1382 cm^{-1} (-N-H); 1153cm^{-1} (skeleton: C-O and –C-O-C) ; 889 cm^{-1} C-O-C bridge as well as glucosidic linkage; 580 and 529 cm^{-1} (Ni-N-); 433cm^{-1} (Ni-O)

The absorption wave number of -C-N- stretching vibration and –N-H- stretching vibration of chitosan-metal ion complexes are smaller than that of chitosan. These results indicate the interaction of NH_2 in chitosan with metal ion forming the chitosan- metal complex.

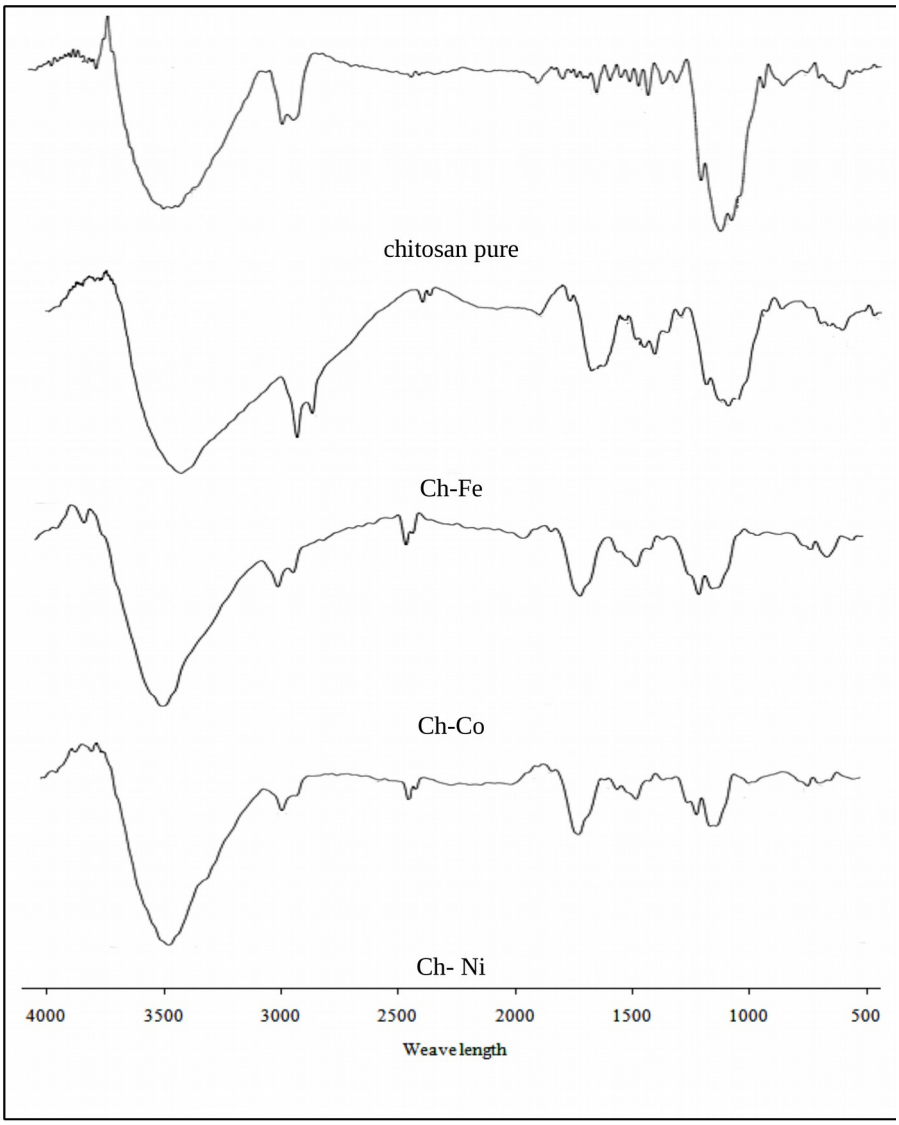

Fig. 4 FT-IR of chitosan and chitosan-metal complexes

Scanning electron microscope

Fig. 5 shows that chitosan has a smooth surface [11-13]. However Fig. 6 shows the Ch-Fe(1) complex has a very smooth surface, the ‘‘holes’’ in such surface are little leads to a strong and specific binding of the amino groups of chitosan with Fe

ions. While Fig. 8 shows the Ch-Ni(1) complex is a less smooth with more holes than Ch-Fe complex due to the weak binding with the amino groups of chitosan.

In Fig. 7 the Ch-Co(1) complex has a different surface structure than other complexes. The significant morphological changes in both chitosan and chitosan-metal complexes indicate the formation of complexes.

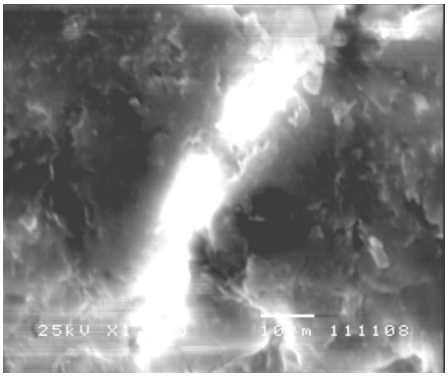

Fig. 5 SEM of prepared pure chitosan

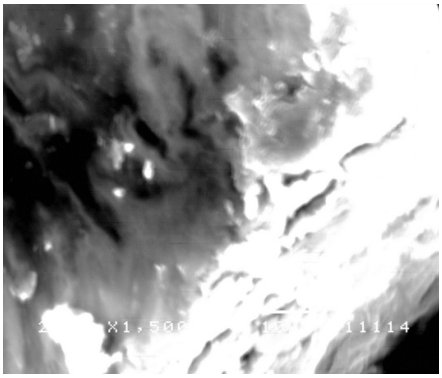

Fig. 6 SEM of Ch-Fe(1) complex

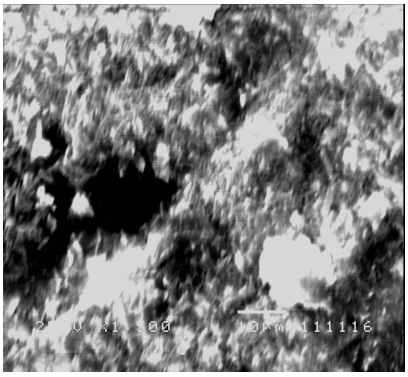

Fig. 7 SEM of Ch-Co(1) complex

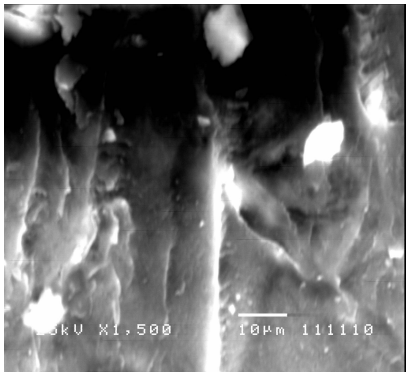

Fig. 8 SEM of Ch-Ni(1) complex

X ray diffraction

Fig.9 shows the XRD patterns of chitosan and chitosan-metal complexes (Ch-Fe, Ch-Ni and Ch-Co) [13, 14, 15]. The specific peaks of chitosan and Ch-Fe complex were observed at diffraction angles of 19º and 22º, respectively, indicating that both chitosan and Ch-Fe complex as were amorphous. However, the Ch-Co has four peaks observed at 32º. 38º, 52º

and 58º, but Ch-Ni has three peaks observed at 33º, 39º and 59º, indicating the crystalline phase structure of Ch-Co and Ch-Ni complexes.

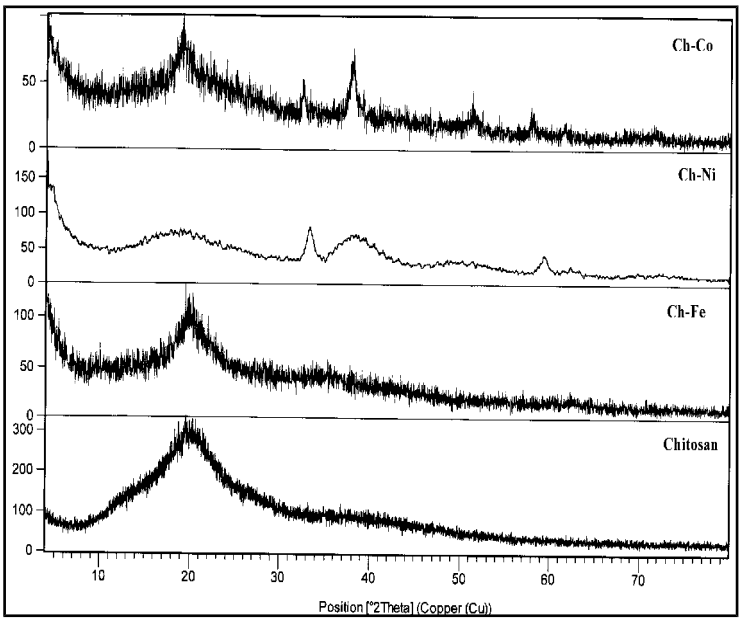

Fig. 9 XRD pattern of chitosan and chitosan-metals complexes.

TGA analysis

Figs. 10-12 show thermal gravimetric analysis (TGA) of chitosan and chitosan-metal complexes (Ch-Fe, Ch-Co, and Ch-Ni) [16] in three different ratios indicated that chitosan and chitosan-metal complexes proceed in two stages: the first stage explained the water weight loss, while the second one is the degradation of chains with greater weight loss, Table (2) shows the weight loss percentages of two stages for chitosan and chitosan-metal complexes.

Table (2): Weight loss percentages of (TGA) curves for chitosan and chitosan-metal complexes.

Sample	*Weight loss (%)*	
	First stage	*Second stage*
Chitosan	10.11	39.86
Ch-Fe(1)	11.4	39.5
Ch-Fe(2)	10.6	38.7
Ch-Fe(3)	7.07	41.4
Ch-Co(1)	7.3	25.6
Ch-Co(2)	6.3	34.3
Ch-Co(3)	13.1	24.1
Ch-Ni(1)	15.7	29.5
Ch-Ni(2)	15.3	32.1
Ch-Ni(3)	11.7	35.3

The entire TGA study demonstrated that the chitosan-metal complexes become less stable than chitosan free due to the effect of complexation between transition metal ions and chitosan molecular chains.

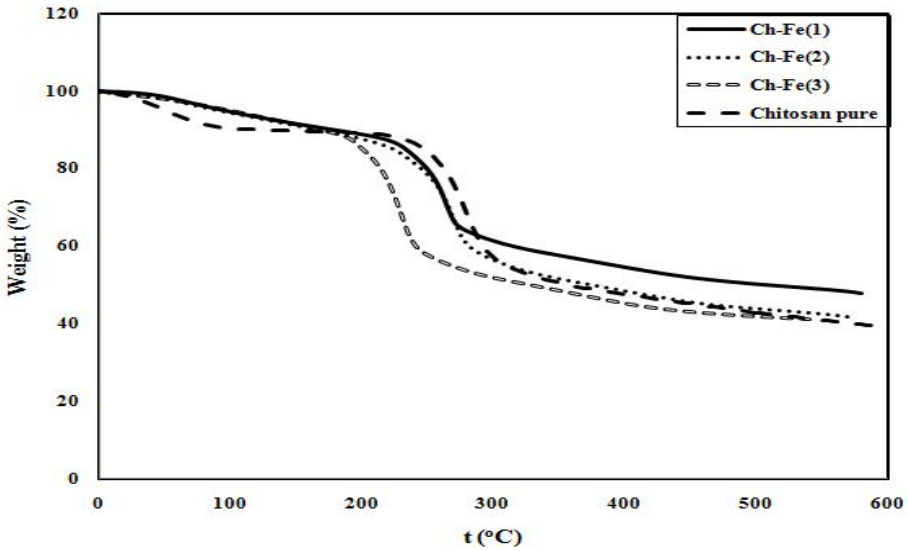

Fig.10: TGA of chitosan and Ch-Fe complexes

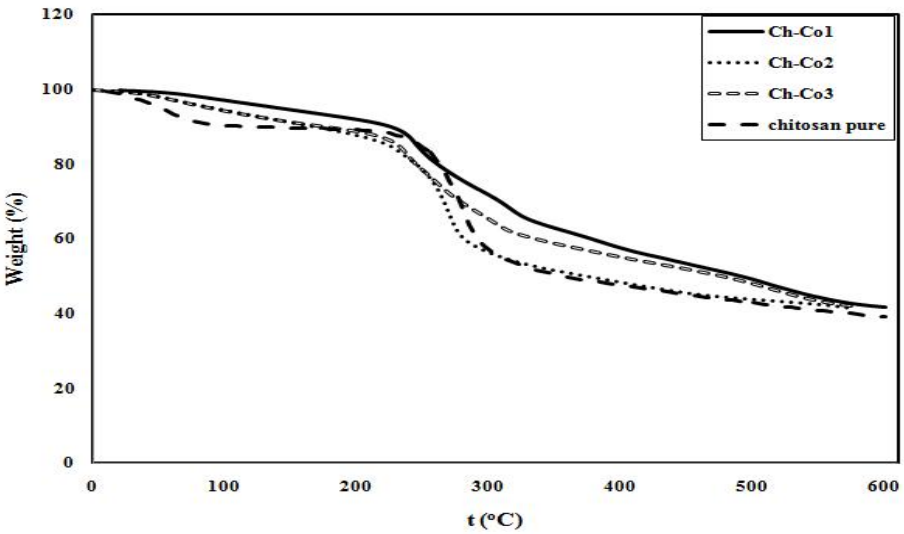

Fig.11: TGA of chitosan and Ch-Co complexes

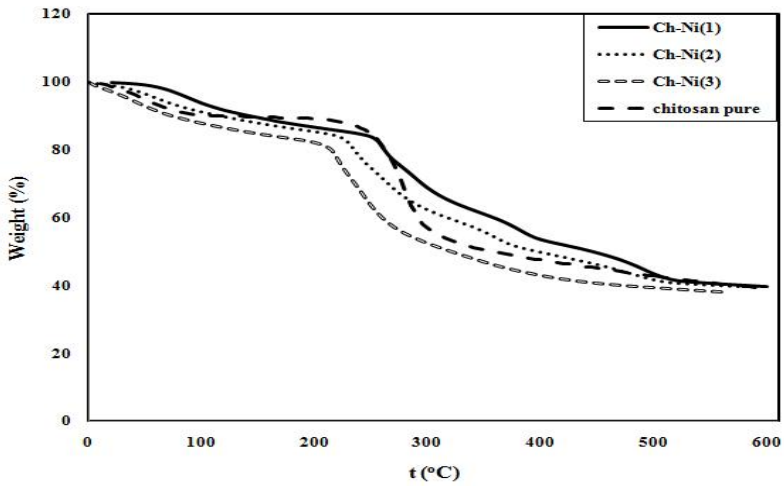

Fig.12 T GA of chitosan and Ch-Ni complexes

DSC curves of chitosan metal ions complexes

The differential scanning calorimetric (DSC) peaks for chitosan and chitosan-metal complexes recorded in nitrogen from 30°C to 700°C are shown in Figs. 13-15

Table (3): The decomposition temperatures of chitosan and chitosan-metal complexes

Sample	*Peaks (°C)*		
	Endothermic	*Exothermic I*	*Exothermic II*
Chitosan	96	298	450
Ch-Fe(1)	100	250	290
Ch-Fe(2)	95	230	275
Ch-Fe(3)	80	195	240
Ch-Co(1)	95	245	292
Ch-Co(2)	91	253	295
Ch-Co(3)	90	265	299
Ch-Ni(1)	105	260	340

Ch-Ni(2)	96	258	309
Ch-Ni(3)	97	259	300

For chitosan the exothermic peak at 298°C, correspond to the decomposition of the high content of amine (GlcN) groups, while the small exothermic peak at 450°C due to the decomposition of acetyl (GlcNAc) units.

For chitosan-metal complexes there are exothermic peaks, and all the peaks shifted thermally to a lower temperature in two degradation states with increasing of the metal ion, indicating that chelation of chitosan with metal ion leads to its thermal instability, these results are well correlated with results of TGA. The temperatures of both endothermic and exothermic peaks for chitosan and chitosan-metal complexes were tabulated in Table (3).

From results in Tables (3,4), in general, we obtain a great evidence that the chitosan-metal complexes thermally less stable than free chitosan, this means that the metal ions act as a catalyst for the degradation of chitosan, also the Ch-Ni complexes are thermally more stable than Ch-Co ones, while the Ch-Fe complexes are thermally less stable.

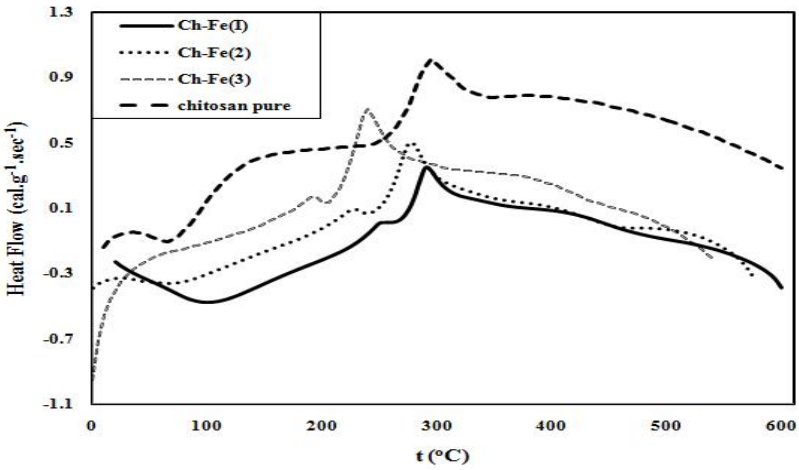

Fig.13 DSC curves of chitosan and Ch-Fe complexes.

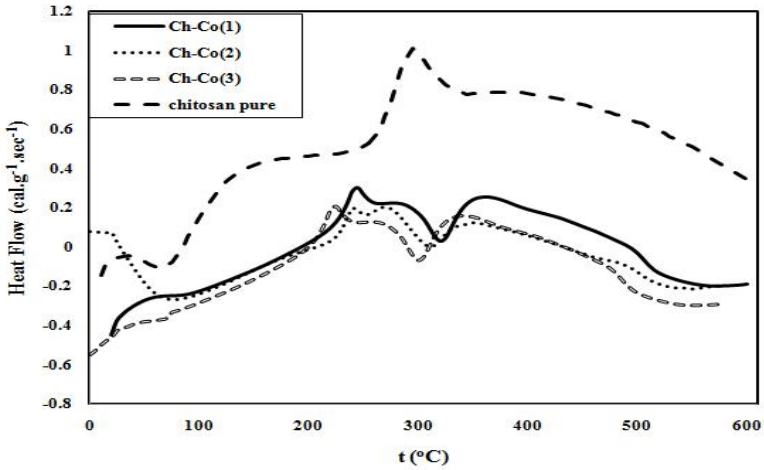

Fig.14 DSC curves of chitosan and Ch-Co complexes.

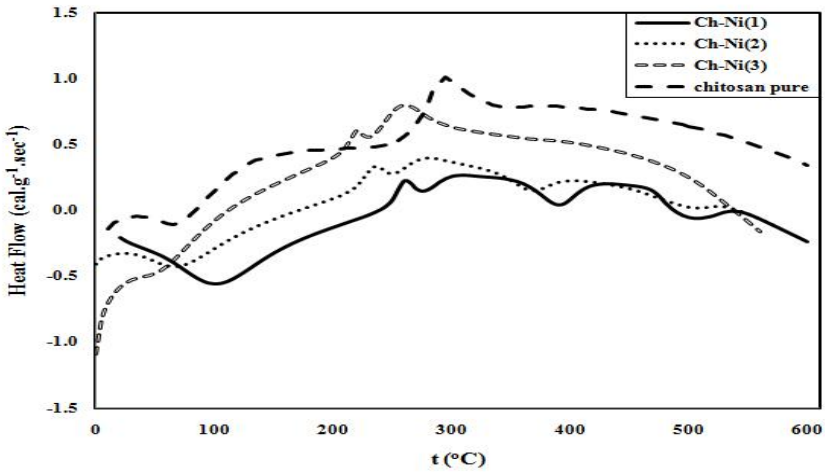

Fig.15 DSC curves of chitosan and Ch-Ni complexes compounds.

Determination of activation energy of decomposition of chitosan and chitosan-metal complexes [16]

The activation energy was determined by the Arrhenius relationship according to Broido method in Eq.1.

$$\ln\left[\ln\left(\frac{1}{1-\alpha}\right)\right] = -\frac{E_a}{RT} + \ln\left[\left(\frac{R}{E_a}\right)\left(\frac{Z}{U}\right)T_m^2\right] \quad (1)$$

where E_a is the activation energy (J mol^{-1}), R is the gas constant (8.314 J $mol^{-1}K^{-1}$) ,T is the absolute temperature (K), T_m is the temperature of the maximum reaction

velocity, Z is a constant, u is the heating rate and α is extent of decomposition calculated according Eq.2.

$$\alpha = -\frac{w_o - w_t}{w_o - w_f} \quad (2)$$

where W_o, W_t and W_f are the initial, actual and final mass of the sample, respectively.

The apparent activation energies (E_a) for the thermal degradation of chitosan and chitosan–metal ions are calculated from the second thermal degradation stages of TGA curves using Broido method, based on Eq.2.

Plots of ln{ln[1/(1-α)]} versus 1/T for all chitosan-metal complexes, are shown in Figs. 16-25. It can be seen that there are two distinct degradation periods. E_a obtained for the two degradation periods are reported in Table (4).

In Period (I), the decomposition of coordination bonds between functional groups of chitosan and metal ions. The activation energy of chitosan-metal complexes increases with decreasing the Fe^{3+}, Ni^{2+} and Co^{2+} ratio, indicated that the catalytic effect of metal ions on decomposition processes, also the activation energy values are higher in case of Ch-Fe complexes than Ch-Ni and Ch-Co complexes, due to the fact that structures of Ch-Fe complexes are more stable than Ch-Ni, while the structures of Ch-Co complexes are less stable [17, 18], according to the stability constant of metal complexes.

Periods (II) the cleavage of glycosidic linkages of chitosan. E_a value of chitosan higher than chitosan-metal complexes, and a decrease of E_a with increasing amount of metal ions, indicate that the conformation change of chitosan, resulted from mixing of metal ions in chitosan and has au effect on the formation of new phases of the polymer, which partly decreases bond energies of glycosidic linkages in chitosan, consequently leads to its partially thermal instability, also the activation energy values for all chitosan complexes decreases with increase of the metal ion ratio indicated that a catalytic effect of metal ions on decomposition processes.

Table (4): The activation energy values of two periods for chitosan and chitosan-metal compounds

Sample	*Period I*		*Period II*	
	E_a (kJ.mol^{-1})	*Z (Sec^{-1}(*	*E_a (kJ.mol^{-1})*	*Z (Sec^{-1}(*
Chitosan	--	--	118.32	0.135

Ch-Fe(1)	110.10	0.13	44.26	0.031
Ch-Fe(2)	117.74	0.15	45.20	0.033
Ch-Fe(3)	144.86	0.20	45.42	0.035
Ch-Co(1)	95.62	0.12	66.14	0.065
Ch-Co(2)	102.36	0.13	71.94	0.060
Ch-Co(3)	114.02	0.14	78.61	0.079
Ch-Ni(1)	106.12	0.13	53.33	0.040
Ch-Ni(2)	112.44	0.14	53.57	0.042
Ch-Ni(3)	121.14	0.16	56.79	0.050

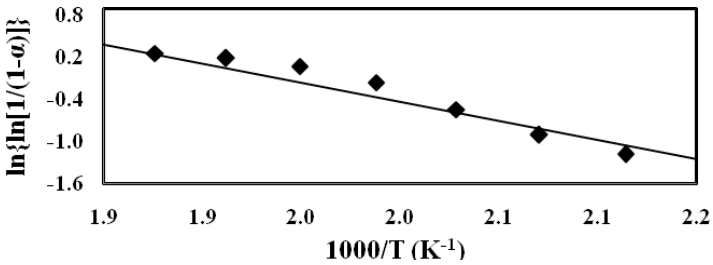

Fig. 16 The ln{ln[1/(1-α)]} vs. 1000/T of the prepared chitosan.

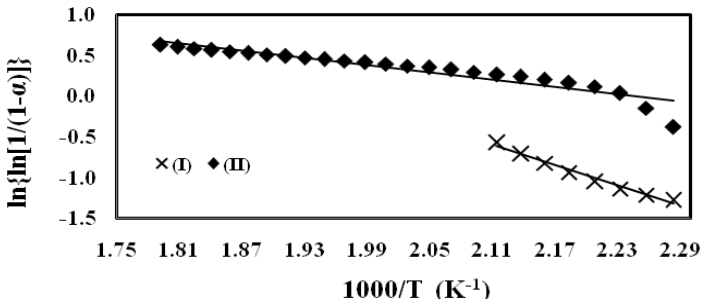

Fig. 17 The ln{ln[1/(1-α)]} vs. 1000/T of Ch-Fe(1) complex.

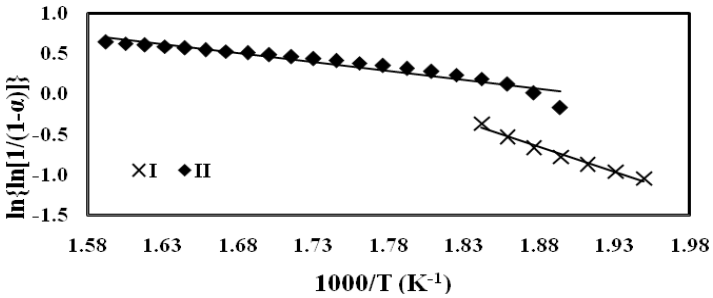

Fig. 18 The ln{ln[1/(1-α)]} vs. 1000/T of Ch-Fe(2) complex.

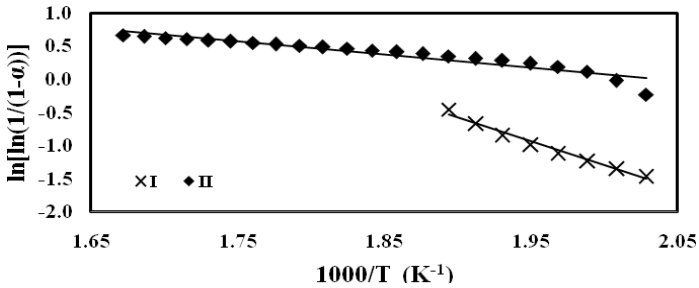

Fig. 19 The ln{ln[1/(1-α)]} vs. 1000/T of Ch-Fe(3) complex.

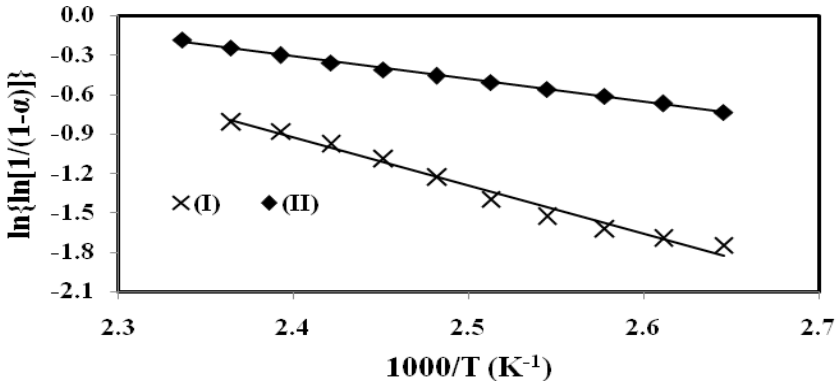

Fig. 20 The ln{ln[1/(1-α)]} vs. 1000/T of Ch-Co(1) complex.

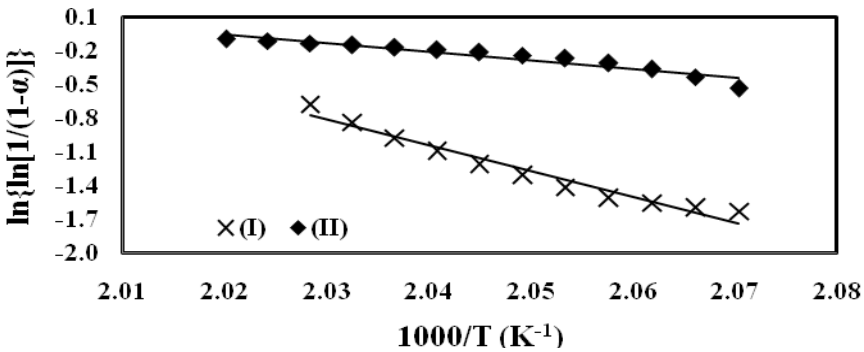

Fig. 21 The ln{ln[1/(1-α)]} vs. 1000/T of Ch-Co(2) complex.

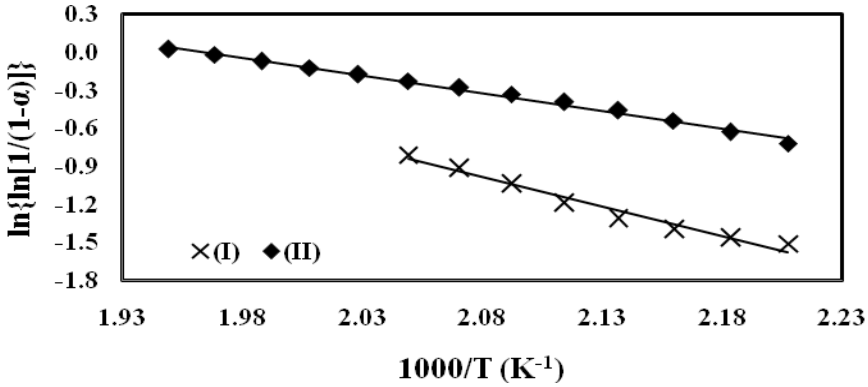

Fig. 22 The ln{ln[1/(1-α)]} vs. 1000/T of Ch-Co(3) complex.

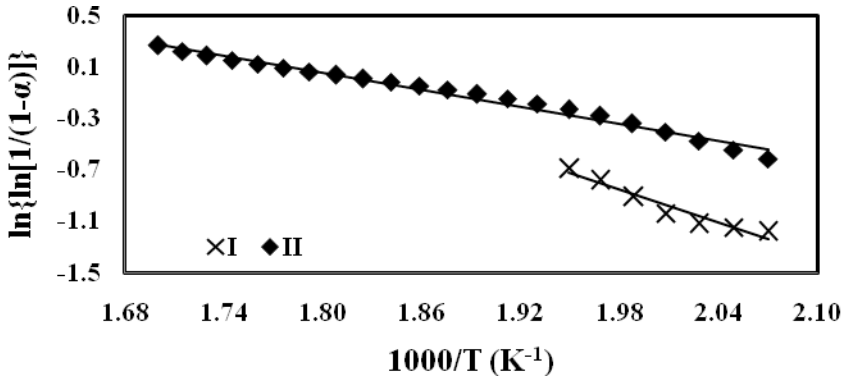

Fig. 23 The ln{ln[1/(1-α)]} vs. 1000/T of Ch-Ni(1) complex.

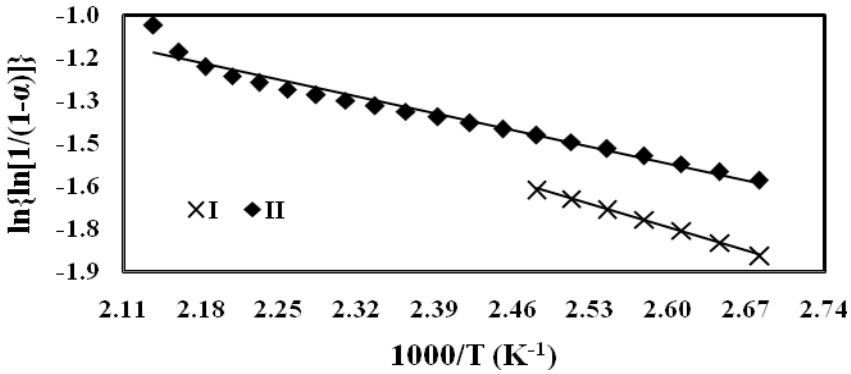

Fig. 24 The ln{ln[1/(1-α)]} vs. 1000/T of Ch-Ni(2) complex.

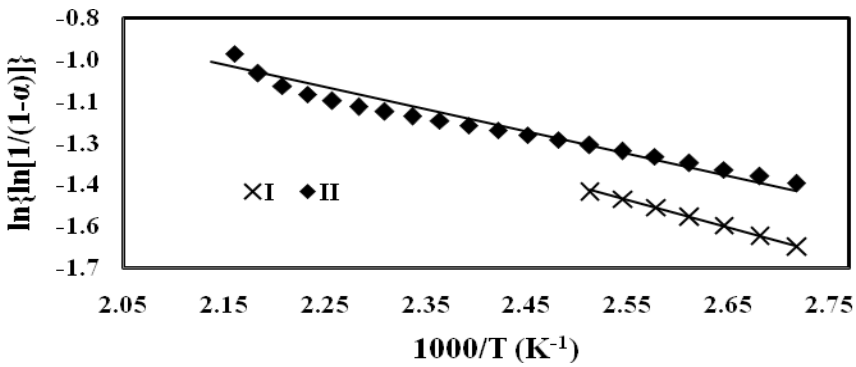

Fig.25 The ln{ln[1/(1-α)]} vs. 1000/T of Ch-Ni(3) complex.

Electrical conductivity measurements of chitosan and chitosan-metals ions complexes [19,20]

The electrical conductivity (σ) was calculated from Eq.3

$$\sigma = \frac{1}{\rho} \tag{3}$$

where ρ is specific resistance of materials and it is calculated from Eq.4.

$$\rho = \frac{(R \times A)}{L} \tag{4}$$

where R is resistance, A is total area and L is the thickness of sample

Effect of metal ions

Table (5) shows the variation in electrical conductivity of chitosan-metal ion complexes at 298 K. The data showed that in general the addition of metal ion causes an increase in electrical conductivity of the chitosan. This result is presumably due to association of the metal cation with polar or charged groups on the polymer, e.g. chelation between the cation and the lone pair of electron in the amino or hydroxy group in the chitosan chain. Such association causes an enhancement in the ionic conductivity of the chitosan matrix. A possible mechanism has been suggested that an ion transport in polyelectrolyte materials proceeds via formation of a transition state, in which a metal ion bind to a particular polar group, associates with a polar group on a new segment of polymer chain, before dissociating it to the old site. This leads to the hopping of ions from one polymer chain to the next. However, the nature of the metal ion, including the size and the valency, can also influence the electrical conductivity of the complex compounds. The ionic conduction mechanism of polyelectrolyte materials is dependent on the mobility of the metal ion, and the interaction between the polymer and the metal ion. Thus, the electrical conductivity of the complex compounds can be varied by changing the type of metal ion. The electrical conductivity of the Ch-Fe complexes exhibits higher values compared to the complexation loaded with Ni^{2+}, and Co^{2+} ions. This result can be explained on the basis the interaction between Fe^{3+} and the electronegative groups in chitosan structure is weaker than the corresponding interaction of Ni^{2+}, and Co^{2+} ions which can even form physical cross-links between OH, and NH_2 groups in the chitosan matrix. This result in a higher mobility of Fe^{3+} in the matrix and consequently a higher conductivity is obtained.

The configuration of Fe^{3+} is ($3p^6\ 3d^5$), when the five 3d orbitals are either singly as doubly filled a degree of stability is established on the atom or ion and thus exhibit a stability to the electronic configuration of $Fe^{3+}(3d^5)$. The Fe^{3+} ion loses easily 2 electrons moving from one chitosan ion to another. Hence the conductivity of product is electronic and not ionic.

Table (5): Conductivity values of chitosan and chitosan-metals complex at 298 K

Sample	***A(cm³)***	***L ×10³ (cm)***	***R ×10⁻¹⁰ (Ω)***	***ρ ×10⁻¹³ (Ω.cm²)***	***σ ×10¹³ (Ω⁻¹.cm⁻²)***
Chitosan	3.14	1.50	31000	720.0	0.0013

Ch-Fe(1)	3.14	2.65	00.44	0.05	192.21
Ch-Fe(2)	3.14	1.65	15.99	3.05	32.81
Ch-Fe(3)	3.14	1.03	24.52	7.84	13.36
Ch-Co(1)	3.14	1.70	25.81	4.77	20.98
Ch-Co(2)	3.14	1.50	30.99	6.49	15.41
Ch-Co(3)	3.14	1.52	316.17	65.42	1.52
Ch-Ni(1)	3.14	4.20	14.65	1.10	91.20
Ch-Ni(2)	3.14	2.12	23.52	3.49	28.76
Ch-Ni(3)	3.14	1.03	45.54	13.90	7.19

References

1. Baraka, A.; Hall, P. J.; Heslop, M. J. J. Hazard. Mater., **140**,(2007) 86–94.
2. Bose, P.; Bose, M. A.; Kumar, S. Adv. Environ. Res., 7, (2002) 179–195.
3. Crini, G. Bioresour. Technol., 60, (2006)67–75.
4. Aksu, Z. Process Biochem., 40, (2005) 997–1026.
5. E. Forgacs, T. Cserhati, G. Oros, Environ. Int., 30, (2004) 953–971.
6. C. A. Kozlowski, W. Walkowiak, Water Res., 36, (2002) 4870–4876.
7. S. Rio, A. Delebarre, Fuel, 82, (2003)153–159.
8. Y. C. wong. Y. S. Szto, W. H. Cheung and G. Mckay., J. Process Biochem. 39 (2004) 693, J. Langmuir 19 (2003) 7888
9. M. R. Kasaai,J. Carbohydrate Polymers 71(2008(497–508.
10. R. B. Hernandez. J. Molecular Structure 877 (2008) 89–99.
11. K. D. Trimukhe, & A. J. Varma, Carbohydrate Polymers, 71 (2008) 66–73, 698–702.
12. C. Demetgu, S, Serin, ibid, 72 (2008) 506–512.
13. H. Liua, Y. Dua, X. Wanga, Y. Hua, J. F. Kennedy, Carbohydrate Polymers 56 (2004) 243–250.
14. X. Wang, Y. Du, L. Fan, H. Liu and Y. Hu, polymer Bulletin 55 (2005)105–113.
15. H. Liu. Int. J. Food Microbiology 95 (2004) 147–155.
16. C. Y. Ou, Si. D. Li, C. P. Li, C. H. Zhang, L. Yang, C. P. Chen J. Applied Polymer Science, 109, (2008) 957–962
17. E. Furia Thomas, Handbook of Food Additives, Chapter 6, 2nd ed. CRC press (1972).

18. G. G. Mohamed. Spectrochimica Acta. Part A 57 (2001) 1643-1648.

19. T. Thanpitcha, A. Sirivat, Alexander, M. Jamieson, R. Rujiravanit. Macromol. Symp. **264** (2008) 168–175.

20. Ernesto Lo´pez Cha´vez, R. Oviedo-Roa, Gustavo Contreras-Pe´rez, Jose´ Manuel Martı´nez-Magadan, F.L. Castillo-Alvarado. International journal of hydrogen energy **35** (2010)12141–12146.